J Antimicrob Chemother 2010; **65**: 2347–2358
doi:10.1093/jac/dkq311 Advance Access publication 1 September 2010

Journal of Antimicrobial Chemotherapy

Targeting the chromosome partitioning protein ParA in tuberculosis drug discovery

Shahista Nisa[1], Marian C. J. Blokpoel[2], Brian D. Robertson[2], Joel D. A. Tyndall[3], Shichun Lun[4], William R. Bishai[4] and Ronan O'Toole[1]*

[1]*School of Biological Sciences, Victoria University of Wellington, Wellington, New Zealand;* [2]*Centre for Molecular Microbiology and Infection, Division of Infectious Diseases, Imperial College London, London, UK;* [3]*National School of Pharmacy, University of Otago, Otago, New Zealand;* [4]*Center for Tuberculosis Research, Department of Medicine, Division of Infectious Diseases, Johns Hopkins University School of Medicine, Baltimore, MD, USA*

*Corresponding author. Tel: +64 -4-463-6088; Fax: +64-4-463-5331; E-mail: ronan.otoole@vuw.ac.nz

Received 4 March 2010; returned 28 April 2010; revised 7 July 2010; accepted 19 July 2010

Objective: To identify inhibitors of the essential chromosome partitioning protein ParA that are active against *Mycobacterium tuberculosis*.

Methods: Antisense expression of the *parA* orthologue MSMEG_6939 was induced on the *Mycobacterium smegmatis* background. Screening of synthetic chemical libraries was performed to identify compounds with higher anti-mycobacterial activity in the presence of *parA* antisense. Differentially active compounds were validated for specific inhibition of purified ParA protein from *M. tuberculosis* (Rv3918c). ParA inhibitors were then characterized for their activity towards *M. tuberculosis in vitro*.

Results: Under a number of culture conditions, *parA* antisense expression in *M. smegmatis* resulted in reduced growth. This effect on growth provided a basis for the detection of compounds that increased susceptibility to expression of *parA* antisense. Two compounds identified from library screening, phenoxybenzamine and octoclothepin, also inhibited the *in vitro* ATPase activity of ParA from *M. tuberculosis*. Structural *in silico* analyses predict that phenoxybenzamine and octoclothepin undergo interactions compatible with the active site of ParA. Octoclothepin exhibited significant bacteriostatic activity towards *M. tuberculosis*.

Conclusions: Our data support the use of whole-cell differential antisense screens for the discovery of inhibitors of specific anti-tubercular drug targets. Using this approach, we have identified an inhibitor of purified ParA and whole cells of *M. tuberculosis*.

Keywords: *Mycobacterium*, tuberculosis, essential gene, cell division, antisense

Introduction

The discovery of streptomycin by Selman Waksman in 1943 was believed to herald the end for tuberculosis,[1] a disease that has afflicted mankind for at least 9000 years.[2] However, recent data from the WHO show that there are more than 9 million new cases of the disease each year.[3] In addition, approximately 0.5 million cases are caused by multidrug-resistant (MDR) forms of *Mycobacterium tuberculosis*, defined as resistant to both isoniazid and rifampicin.[3,4] The prevalence of MDR tuberculosis is considered a threat to global control programmes as it necessitates an extended and more costly treatment regimen for which the success rate is reduced considerably.[5,6] In March 2006, the CDC reported the appearance of extensively drug-resistant (XDR) strains of *M. tuberculosis*,[7] defined as resistant to both isoniazid and rifampicin, one of the fluoroquinolones and one injectable aminoglycoside.[8] According to the WHO, XDR tuberculosis 'leaves patients (including many people living with HIV) virtually untreatable using currently available anti-tuberculosis drugs'.[9] From an initial detection in the USA, South Korea and Latvia in 2006, 58 countries have confirmed at least one case of XDR tuberculosis.[10]

New tuberculosis drugs are required to meet the WHO target of halving the global incidence of tuberculosis.[11] The current anti-tubercular therapy inhibits primarily DNA synthesis (fluoroquinolones), transcription (rifampicin), translation (aminoglycosides) and cell wall biosynthesis (isoniazid, ethambutol).[12] To develop more effective antibiotics for treating tuberculosis, alternative targets are needed.[13–15] The publication of the *M. tuberculosis* genome sequence made it possible for researchers

to begin selecting other mycobacterial processes for the discovery of new candidate drugs.[16,17] Genes essential for basic cellular processes in bacteria represent potential targets for anti-infective therapy as their genetic or chemical inactivation can halt bacterial growth. Cell division, although an essential process in all living organisms, is markedly different in prokaryotes and eukaryotes[18–20] and has received only modest attention for antibacterial drug discovery to date.[21,22] Its promise as a source of new drug targets is supported by the recent discovery of zantrins, antagonists of the cell division protein FtsZ, which are active against several clinically important bacterial pathogens, including methicillin-resistant *Staphylococcus aureus* (MRSA), *Streptococcus pneumoniae*, *Shigella dysenteriae*, *Vibrio cholerae*, *Escherichia coli* and *Clostridium perfringens*.[21]

The discovery of new tuberculosis drugs is dependent on assays that can reliably identify anti-mycobacterial compounds in high throughput. A number of high-throughput screen (HTS) protocols are based on inhibition of a specific purified protein. For example, White *et al.*[23] used the rate of ATP utilization by pantothenate synthetase (PS) to identify inhibitors of *M. tuberculosis* PS, an essential enzyme for coenzyme A and acyl carrier protein biosynthesis. Bhat *et al.*[24] used the incorporation of a fluorescent analogue of uridine monophosphate (UMP) into nascent RNA to perform HTS for inhibitors of RNA polymerase of *E. coli* and validated hits against the RNA polymerases of *Mycobacterium smegmatis* and *Mycobacterium bovis*.[24] While these assays can detect inhibitors of specific enzymes, they are unable to eliminate compounds that have poor permeability with respect to entry into the mycobacterial cell. On the other hand, whole-cell assays address the issue of compound permeability; however, they do not provide information on the cellular target of the inhibitors detected.

To overcome the above challenges, we set up a whole-cell assay to enable detection of inhibitors of a protein that is required in the mycobacterial cell division process, ParA.[25] The assay consisted of a differential sensitivity screen for compounds that act synergistically with *parA* antisense expression. Using this approach, compounds that enhanced the inhibitory effect of *parA* antisense expression of *M. smegmatis* were identified from chemical libraries. These compounds were validated using purified ParA protein and tested for activity against *M. tuberculosis*.

Methods

Bacterial strains and growth conditions

E. coli DH5α and *E. coli* BL21 (DE3) were cultured in Luria-Bertani broth (LB) and on Luria-Bertani agar (LA). *M. smegmatis* mc^2155 was cultured in LB supplemented with 0.1% Tween 80 (LBT) and on LA. *M. bovis* BCG and *M. tuberculosis* H37Ra were cultured in Middlebrook 7H9 broth supplemented with 10% (v/v) OADC (0.06% oleic acid/5% BSA/2% dextrose/0.85% NaCl), 0.5% (v/v) glycerol and 0.1% (v/v) Tween 80. *M. tuberculosis* H37Rv and CDC1551 were cultured in Middlebrook 7H9 broth supplemented with 10% (v/v) OADC, 0.2% (v/v) glycerol and 0.05% (v/v) Tween 80. Nutrient-limitation assays of *M. smegmatis* were conducted using Hartman-de Bonts (HdeB) minimal medium as previously described.[26,27] All strains were cultured at 37°C.

Construction of a conditional antisense expression vector

M. smegmatis genomic DNA was extracted as previously described[28] and used as a template for PCR amplification of the full-length open reading frames of MSMEG_2357, MSMEG_6938 and MSMEG_6939. PCR experiments were carried out as per the manufacturer's instructions with the following primers: MSMEG_2357_F (5′-CTAGTTAATTAACTGCAACTG CCCGGTGAC-3′) and MSMEG_2357_R (5′-CTAGTTAATTAATCATCGGCTCA CCGTCCC-3′) for MSMEG_2357 antisense; MSMEG_6938_F (5′-CTAG ACTAGTATGAATCAGCCGGCACGCAA-3′) and MSMEG_6938_R (5′-CTAG CATATGTTACTCGTTCTGGGCGCTCA-3′) for MSMEG_6938 antisense; MSM EG_6939_F (5′-CTAGGATATCATGGGTTCGGGTCAGAACAA-3′) and MSMEG_ 6939_R (5′-CTAGGATATCCTACTGCTGGCGCGGCGGCG-3′) for MSMEG_6939 antisense. MSMEG_6939_F and MSMEG_6938_R were used to generate the combined MSMEG_6938+6939 antisense fragment. The endonuclease restriction sites in the primers are underlined. For the analysis of PCR-amplified DNA fragments, the TA cloning vector pCR2.1 (Invitrogen) was used and recombinants were selected using blue/white colony screening on LA supplemented with 200 mg/L ampicillin, 50 mg/L kanamycin, 100 mg/L IPTG and 40 mg/L 5-bromo-4-chloro-3-indolyl-β-D-galactopyranoside (Xgal). Pure colonies were cultured in LB supplemented with 200 mg/L ampicillin and 50 mg/L kanamycin.

A modified version of the mycobacterial expression vector pMind containing the *tetR* gene and *tetO* operator from *Corynebacterium glutamicum* was used to induce antisense gene expression as previously described.[29] pHS201[30] was used as a template for PCR amplification of the green fluorescent protein (*gfp*) gene using primers GFP_RBS_F (5′-CTAGACTAGTTTTAAGAAGGAGATATACATATGAGTAAAGGAGGA-3′) and GFP_R (5′-CTAGACTAGTTTATTATTTGTATAGTTCATCCATGCC-3′). The *gfp* gene was inserted into the SpeI site of the pMind vector downstream of the *tetO* operator, generating pMindGFP (Figure 1). The orientation of fragments in pMind was determined by PCR using a primer complementary to the *tetO* operator, TetRO-F11 (5′-CTTCCGGTGGTGAGTCATAG-3′), and the forward and reverse primers were used to generate the fragment. In addition, a primer complementary to the hygromycin resistance gene, HygR11 (5′-AAGTAACAGGGATTCTTGTGTCAC-3′), was used together with the forward and reverse primers. pMindGFP containing the antisense fragments of MSMEG_2357, MSMEG_6938, MSMEG_6939 and MSMEG_6938+6939 was electroporated into *M. smegmatis* using a Bio-Rad Gene Pulser II instrument. Transformants were incubated at 37°C overnight and selected on LA supplemented with 50 mg/L kanamycin and 50 mg/L hygromycin.

Bacterial growth assays

Growth assays of *M. smegmatis*/pMindGFP, *M. smegmatis*/pMind2357, *M. smegmatis*/pMind6938GFP and *M. smegmatis*/pMind6939GFP were conducted in nutrient-rich (LBT) and nutrient-limited (HdeB) media. For nutrient-limitation assays, starter cultures were grown overnight in HdeB media containing 0.2% (v/v) glycerol. For the carbon-limitation assays, the starter cultures were subcultured into HdeB medium supplemented with 0.08% (v/v) glycerol. For the nitrogen-limitation assays, glycerol was present at 0.2% (v/v) and the $(NH_4)_2SO_4$ concentration was reduced 100-fold to 0.15 mM. Each growth assay was performed in quintuplicate in 96-well plates in a total volume of 100 μL with an initial optical density at 590 nm (OD_{590}) of 0.01 (equivalent to an OD_{600} of approximately 0.05 in a 10 mm path length cuvette). For induction of antisense, 0.02 mg/L tetracycline was added. The cultures were monitored for OD_{590} and fluorescence using a Wallac Envision plate reader (Perkin-Elmer). Samples of the cultures were taken at different timepoints, serially diluted and plated onto LA medium to determine the cfu of the cultures.

Differential antisense sensitivity screening of chemical libraries

The *M. smegmatis*/pMind6939GFP strain was screened against two compound libraries: LOPAC (Sigma-Aldrich) and Spectrum Collection

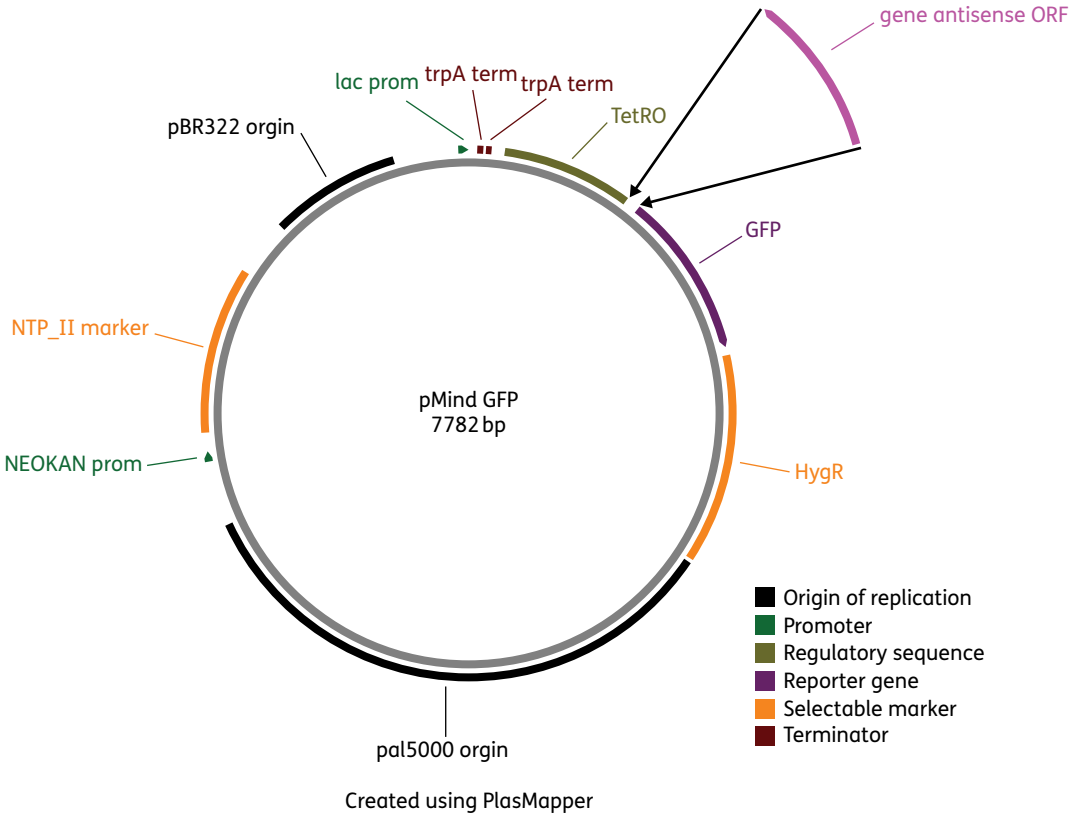

Figure 1. pMindGFP vector map showing the placement of the open reading frame of the target gene in the antisense orientation (pink) downstream of the *tetR* gene and *tetO* operator (green). Addition of tetracycline is used to induce expression. The GFP gene (purple) was cloned downstream of the antisense gene fragment to detect gene antisense expression. Vector map created using PlasMapper.[68] This figure appears in colour in the online version of *JAC* and in black and white in the print version.

(Microsource Discovery Systems) in nutrient-rich and carbon- and nitrogen-limited growth conditions as previously described.[31] Tetracycline was present at a concentration of 0.02 mg/L for induction of antisense expression. Starter cultures were subcultured in 96-well plates to a starting OD_{590} of 0.07 and library compounds were applied at a final concentration of 20 μM in a volume of 100 μL as previously described.[31] Plates were sealed with plate seals, wrapped in cling film and incubated at 37°C until after the cultures reached stationary phase: 72 h for carbon- and nitrogen-limited conditions and 144 h for nutrient-rich conditions. All screens were performed three times. Parallel screens were performed with a reference strain expressing antisense of a putative essential gene, MSMEG_2357, which is not involved in cell division. *M. smegmatis*/pMind2357 strain displayed growth patterns that were similar to *M. smegmatis*/pMind6939GFP (data not shown). Compounds that inhibited both strains in the library screen were excluded. Compounds exhibiting greater than 40% growth inhibition of the *M. smegmatis*/pMind6939GFP strain with respect to the reference strain in all three screens were selected for further characterization. Z-factors were calculated for each screen to determine the fidelity of the assays.

Overexpression of ParA and ParB from M. tuberculosis

M. tuberculosis genomic DNA was extracted as previously described[28] and used as a template for PCR amplification of the Rv3917c (*parB*) and Rv3918c (*parA*) genes. PCR experiments were carried out as per the manufacturer's instructions with the following primers: ParB_F (5′-CTAG AGATCTATGACCCAGCCGTCACGCAG-3′) and ParB_R (5′-CTAGAAGCTT TTACAGAGCGTCCCTGTGCA-3′) for Rv3917c; and ParA_F (5′-CTAGAGATCT GTGAGTGCTCCGTGGGGCCC-3′) and ParA_R (5′-CTAGAAGCTTTCATGGTCG TCCCTTCGCGG-3′) for Rv3918c. The endonuclease restriction sites in the primers are underlined. Analysis of PCR-amplified DNA fragments was carried out using the TA cloning vector pCR2.1, as described above. The *M. tuberculosis* genes were subcloned from the pCR2.1 vectors into the BamHI and HindIII sites of the pET-28a(+) plasmid (Novagen) to generate pET-28a(+)_ParA and pET-28a(+)_ParB. These vectors were transformed into *E. coli* BL21 (DE3) and selected for on LA plates supplemented with 50 mg/L kanamycin. *E. coli* BL21 (DE3)/pET-28a(+)_ParA and *E. coli* BL21 (DE3)/pET-28a(+)_ParB were cultured overnight in LB supplemented with 50 mg/L kanamycin. Protein expression was induced by subculturing 1 mL of the overnight cultures into 500 mL of ZYP-5052 autoinduction medium.[32] The cultures were grown overnight and cells were harvested using centrifugation. Protein purification was carried out using a HisBind Purification kit (Novagen) except the cells were lysed by sonication in 30 mL binding buffer (Novagen). All buffers used for the purification of ParA were supplemented with 10% glycerol. Dialysed ParA protein was stored in 50% glycerol at −20°C.

In silico structural analyses of interactions between inhibitors and ParA

A homology model of *M. tuberculosis* ParA (NCBI Reference Sequence: NP_218434.2) was generated using Modeller 9v7.[33] The sequence of ParA was used as a BLAST search query of the Protein Data Bank, and this resulted in multiple hits with the pdb2BEJ giving the lowest E-value

[E-value, 4.55822e−48; identity, 118/255 (46%)]. A sequence alignment was carried out via the T-coffee (v7.38) webserver (http://www.igs.cnrs-mrs.fr/Tcoffee/tcoffee_cgi/index.cgi). Five models (residues G82–P341; magnesium ion and four coordinated water molecules) were generated from the alignment and the model with the lowest objective function was chosen for docking studies. Low-energy ligand structures were either generated using OMEGA2 and protonated using filter (Openeye software www.eyesopen.com) or were generated in SYBYL-X using the sketcher module (SYBYL-X, Tripos International, St Louis, MO, USA). These ligands were energy-minimized to a low-energy starting conformation using the Tripos forcefield. Flexible ligand docking was carried out with Gold 4.1[34] using the ChemScore scoring function. Threonine-100 was designated as the centre of the ligand binding site with a radius of up to 15 Å. The metal ion was designated as octahedral and all other parameters were default. Graphics were generated using the PyMOL Molecular Graphics System, Version 1.2r3pre.

Development of a ParA ATPase assay and validation of ParA inhibitors

An initial biochemical assay was set up with 50 mM Tris-HCl (pH 7.5), 50 mM KCl, 10 mM $MgCl_2$, 1 mM dithiothreitol (DTT), 0.1 mg/mL BSA, 1 mM ATP, 3 μg ParA, 3 μg ParB and 1 μg *parS* DNA in a total volume of 100 μL. The *parS* region was amplified from *M. tuberculosis* with primers ParS_H37Rv_F (5′-AGATCGATCGTCGCCGGGAT-3′) and ParS_H37Rv_R (5′-GTCTCGAGAGCGGAGAATGT-3). The reaction was incubated for 1 h at 37°C and quantification of inorganic phosphate (P_i) release was used to determine ATPase activity as previously described.[35] Briefly, 20 μL of Reagent A [4.2% (w/v) ammonium molybdate in 4 M sulphuric acid] was added to the ATPase assay followed by 20 μL of Reagent B [0.045% (w/v) brilliant green in H_2O]. The assay reagents were mixed and the reaction was read after 2–5 min at 650 nm. The effects of temperature, presence of divalent cations and presence of ParB and *parS* were also tested in this assay. For validation of the activity of the inhibitors towards ParA, the standard ATPase reactions contained 50 mM Tris-HCl (pH 7.5), 50 mM KCl, 1 mM $MgCl_2$, 1 mM DTT, 100 mg/L BSA, 50 μM ATP and 1 μg of ParA in a total volume of 100 μL. The reaction mixtures were incubated at 37°C for 3 h and ATPase activity was measured as described above.

DAPI staining of M. smegmatis cells

The effects of the validated ParA inhibitors on *M. smegmatis*/pMindGFP and *M. smegmatis*/pMind6939GFP cells were determined under nitrogen-limitation conditions in the presence of 0.02 mg/L tetracycline. Cell morphology and DNA localization were determined by fluorescence microscopy following staining of the cells with 4′,6-diamidino-2-phenylindole (DAPI; Molecular Probes) as per the manufacturer's instructions. Cell lengths were derived from the mean of 100 cells for each culture ± standard error.

Effect of ParA inhibitors on M. smegmatis, M. bovis BCG and M. tuberculosis cells

The effects of validated ParA inhibitors were tested on *M. smegmatis*, *M. bovis* BCG and *M. tuberculosis* H37Ra. Cells were cultured to mid-logarithmic phase and diluted to a starting OD_{590} of 0.01. Sterile deionized water (200 μL) was added to each well on the perimeter of the plate to minimize evaporation of the growth medium during the assay. Growth medium (50 μL) was added to the remaining wells. Starting at 1 mM, 2-fold serial dilutions were performed for the experimental compounds and control antibiotics. Cell culture (50 μL) was added to each inner well, except the medium control wells. The plates were sealed, wrapped in cling film and incubated at 37°C with 200 rpm shaking for 4 days for *M. smegmatis* and 14 days for the slow-growing mycobacteria. At the end of each assay, the OD_{590} of the cultures was measured and the data were analysed with SigmaPlot 11 (Systat) using four-parameter logistic standard curve analysis. The MIC_{90} values were determined with respect to controls. The effects of the ParA inhibitors were also validated in virulent *M. tuberculosis* strains H37Rv and CDC1551. Briefly, the laboratory strain H37Rv and the clinical isolate CDC1551 were grown to mid-log phase and cultures were diluted to an OD_{600} of 0.001 in 7H9 without Tween 80. MICs were determined by the microplate Alamar Blue assay (MABA). Diluted culture (100 μL) containing approximately 10^4 cfu was added to each well containing either serially diluted inhibitors or isoniazid control. Plates were incubated at 37°C for 7 days and 35 μL of Alamar Blue/Tween 80 (2:1.5, v/v) was added to each well and the wells were incubated for 16 h. Plates were read at 544ex/590em with the Optima microplate reader (BMG) and MIC_{90} values were determined.

Results

Introduction of antisense expression vectors into M. smegmatis

The antisense expression vectors were introduced into *M. smegmatis* by electroporation. *M. smegmatis* containing pMind6938GFP or pMind6939GFP formed 1–3 mm colonies on solid medium after 72 h (Figure 2a). In contrast, *M. smegmatis* containing the pMind6938 + 6939GFP vector took approximately 2 weeks to form 1–3 mm colonies on solid medium and was not used in further studies. The *M. smegmatis*/pMind6938GFP and *M. smegmatis*/pMind6939GFP strains were analysed for GFP expression with and without tetracycline. The observed GFP expression in the absence of tetracycline (Figure 2b) indicates that the tetracycline-inducible system on pMindGFP is not tightly regulated. A similar observation has been reported previously for a tetracycline-inducible system used in *Staphylococcus aureus*.[36] The basal expression may account for the severe growth retardation that was observed for *M. smegmatis* containing the antisense fragments for both MSMEG_6938 and MSMEG_6939 (Figure 2a). However, addition of tetracycline resulted in a significantly higher level of GFP fluorescence (Figure 2b), which was indicative of induction of expression from the *tetO* operator on pMindGFP.

Effect of antisense expression on M. smegmatis

The bacterial growth assays were carried out over a period of 300 h and the OD_{590} values of the cultures were measured at regular intervals. All cfu data were compared with data for the *M. smegmatis*/pMindGFP control strain. Under nutrient-rich conditions, induction of antisense expression did not significantly affect the optical density of the cells (Figure 3a). However, there was an ∼300-fold decrease in the cfu at the late stationary phase in *M. smegmatis*/pMind6939GFP with respect to the control strain *M. smegmatis*/pMindGFP (Figure 3b). Under the carbon-limitation conditions, induction of MSMEG_6939 antisense resulted in *M. smegmatis*/pMind6939GFP cultures taking longer to enter stationary phase and this was accompanied by a 14-fold decrease in cfu in *M. smegmatis*/pMind6939GFP cultures (Figure 3c and d). Under nitrogen-starvation conditions, induction of antisense significantly lowered the growth rate and cfu count of the *M. smegmatis*/pMind6939GFP strain (Figure 3e and f). Expression of MSMEG_6939 antisense under nitrogen starvation conditions also affected cell morphology.

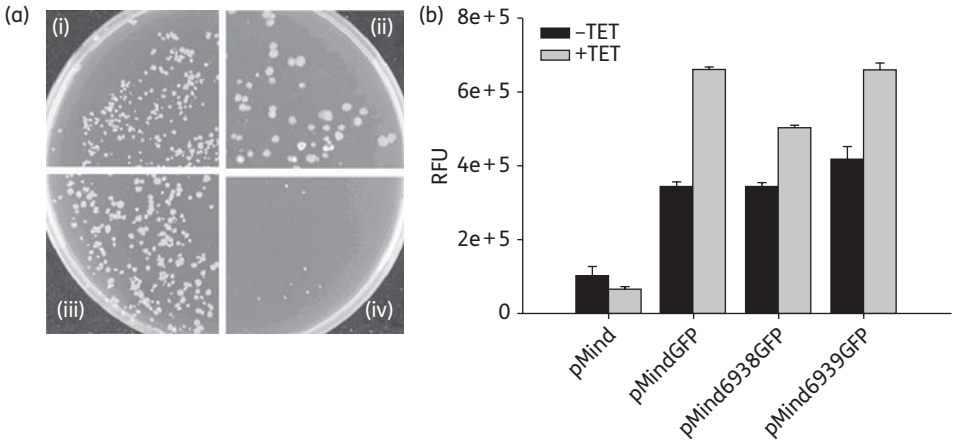

Figure 2. (a) Growth of *M. smegmatis* on agar at 72 h following electroporation with (i) pMindGFP, (ii) pMind6938GFP, (iii) pMind6939GFP and (iv) pMind6938+6939GFP. Electroporations were performed in triplicate in two independent experiments, yielding similar results. The results of one of these independent experiments are shown. (b) Induction of *tetO* operator by addition of 0.02 mg/L tetracycline (TET) as measured by GFP fluorescence. RFU, relative fluorescence units. Results are mean values of triplicates ± standard error.

The *parA* antisense-expressing cells had multiple chromosomal foci along the length of the cells (see Figure 6b) compared with control cells (see Figure 6a). Induction of *parB* antisense expression did not significantly affect the growth or cfu of the *M. smegmatis*/pMind6938GFP strain under any of the culture conditions tested.

Differential antisense sensitivity screen for inhibitors of parA

M. smegmatis containing the *parA* antisense-expressing vector pMind6939GFP was used in a screen of the LOPAC and Spectrum chemical libraries to detect compounds that may inhibit ParA. *M. smegmatis*/pMind6939GFP was grown under nutrient-rich, carbon-limitation and nitrogen-limitation conditions and Z-factors for positive control ethambutol in these screens were 0.90, 0.82 and 0.88, respectively. *M. smegmatis*/pMind6939GFP displayed hypersensitivity towards 44 distinct compounds out of the 3280 library compounds screened. Fourteen compounds were detected under nutrient-rich culture conditions, 5 under carbon limitation and 25 under nitrogen limitation. Of these compounds, seven [AA-861, amsacrine hydrochloride, fenoldopam bromide, R-(−)-fluoxetine hydrochloride, methiothepin mesylate, (±)-octoclothepin maleate and phenoxybenzamine hydrochloride] also induced an elongated cell phenotype in the library screens with the *parA* antisense-expressing strain.

In vitro characterization of ParA from M. tuberculosis

The bacterial ParA protein belongs to a family of P-loop (Walker A box) ATPases.[37] An analysis of the sequence of the ParA protein of *M. tuberculosis* encoded by Rv3918c using the Conserved Domain Database (http://www.ncbi.nlm.nih.gov/Structure/cdd/cdd.shtml) predicts the presence of a P-loop ATPase domain. To test ParA from *M. tuberculosis* for ATPase activity, the protein was expressed in *E. coli* and purified. It was found to hydrolyse ATP in the absence of ParB and *parS* (Figure 4a). The influences of other parameters on the ATPase activity of ParA at saturating ATP concentration were also investigated. Optimal activity was achieved at 37°C. Mg^{2+} was found to stimulate the ATPase activity of ParA significantly more than the other cations tested, Ca^{2+} and Mn^{2+}, with optimal activity at 1 mM Mg^{2+} (data not shown). ATPase activity measured against varying quantities of ParA and at different timepoints showed a linear correlation between 0.5 and 3.0 μg ParA and between 2 and 4 h, respectively. Hydrolysis of ATP by the *M. tuberculosis* ParA ATPase was found to follow Michaelis–Menten kinetics, yielding a K_{cat} and K_m of $22.57 \pm 2.64\ h^{-1}$ and 0.2 ± 0.07 mM, respectively (Table 1). This activity was inhibited by the P-loop ATPase inhibitor metavanadate by approximately 50% at concentrations of 100 μM and higher (Figure 4c).

Inhibition of the ATPase activity of ParA

The optimized ATPase assay was subsequently used to validate seven compounds from the chemical library screens that inhibited the growth of and induced an elongated cell phenotype in the *parA* antisense-expressing strain. Three of these compounds, methiothepin mesylate, (±)-octoclothepin maleate and phenoxybenzamine hydrochloride, showed inhibition in the *in vitro* ParA ATPase assay. Increasing concentrations of phenoxybenzamine progressively decreased the activity of ParA ATPase up to 50% at a concentration of 250 μM (Figure 4d). Concentrations of phenoxybenzamine greater than 250 μM resulted in precipitation of the compound, which interfered with colour development in the Malachite Green assay. Phenoxybenzamine appears to be a mixed inhibitor of ParA, suggesting that it can bind to both the enzyme and the enzyme–substrate complex (Table 1). Addition of octoclothepin resulted in an ∼20% decrease in the ParA ATPase activity at a concentration of 25 μM and higher (Figure 4d). Octoclothepin appears to be a competitive inhibitor of ParA whereby the substrate binding affinity of ParA decreases in the presence of the inhibitors (Table 1). Methiothepin, which is very similar in structure to octoclothepin, yielded nearly identical ParA inhibition results to octoclothepin (data not shown). The standard tuberculosis drugs ethambutol

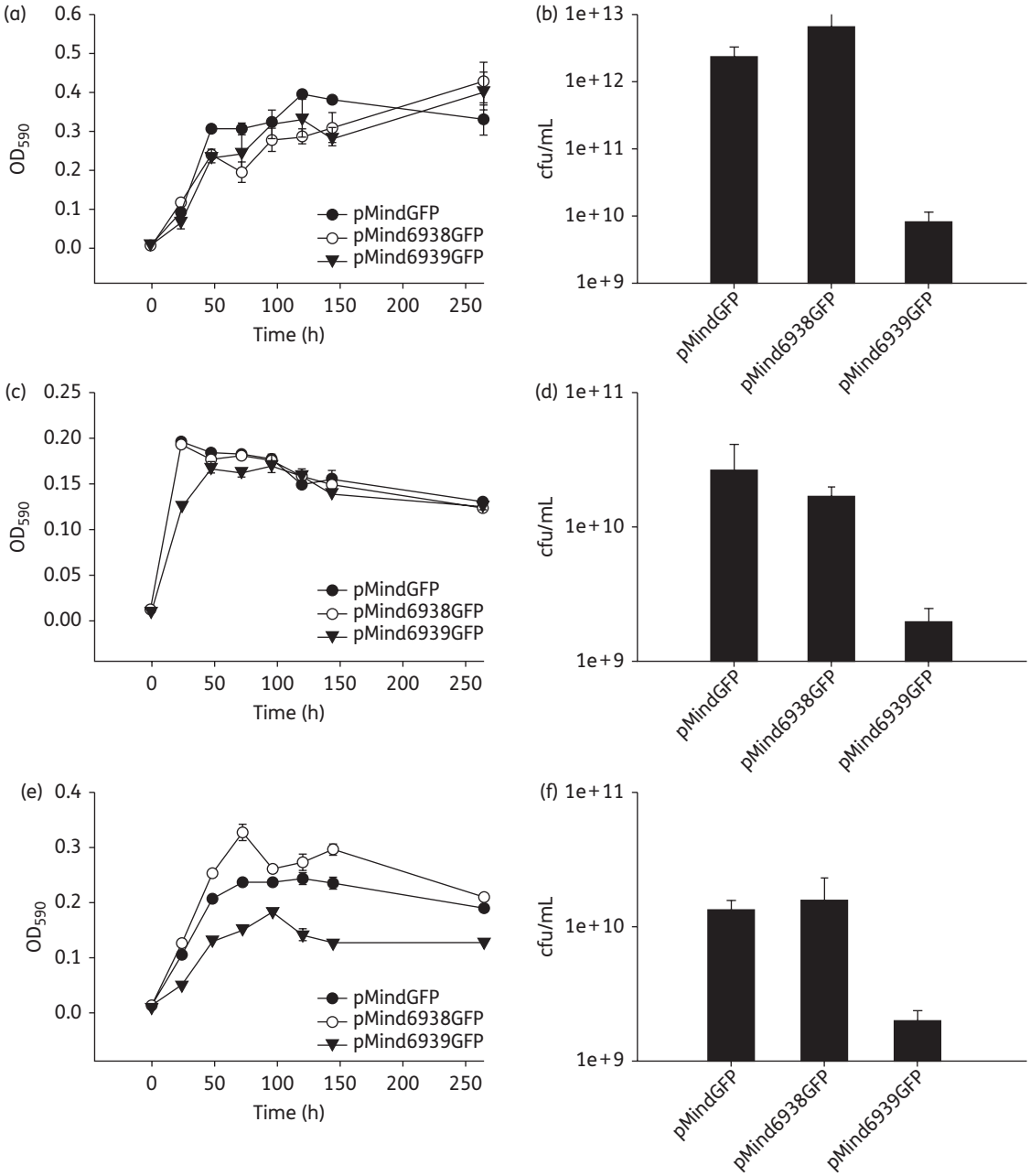

Figure 3. Growth of *M. smegmatis* containing pMindGFP, pMind6938GFP and pMind6939GFP under (a) nutrient-rich, (c) carbon-limitation and (e) nitrogen-limitation conditions as measured by optical density at 590 nm (OD_{590}). Viability of *M. smegmatis* containing pMindGFP, pMind6938GFP and pMind6939GFP under (b) nutrient-rich, (d) carbon limitation and (f) nitrogen limitation conditions as determined by cfu counts. Each growth assay was performed in 96-well plates in a total volume of 100 μL with an initial optical density at 590 nm (OD_{590}) of 0.01 (equivalent to an OD_{600} of approximately 0.05 in a 10 mm path length cuvette). Cultures were incubated at 37°C in 96-well plates and cfu measurements were performed on the cultures after entry into stationary phase: 72 h for carbon- and nitrogen-limited conditions and 144 h for nutrient-rich conditions. Two independent experiments were conducted in quintuplicate yielding similar results. The results of one of these independent experiments are shown. Mean values ± standard error are illustrated.

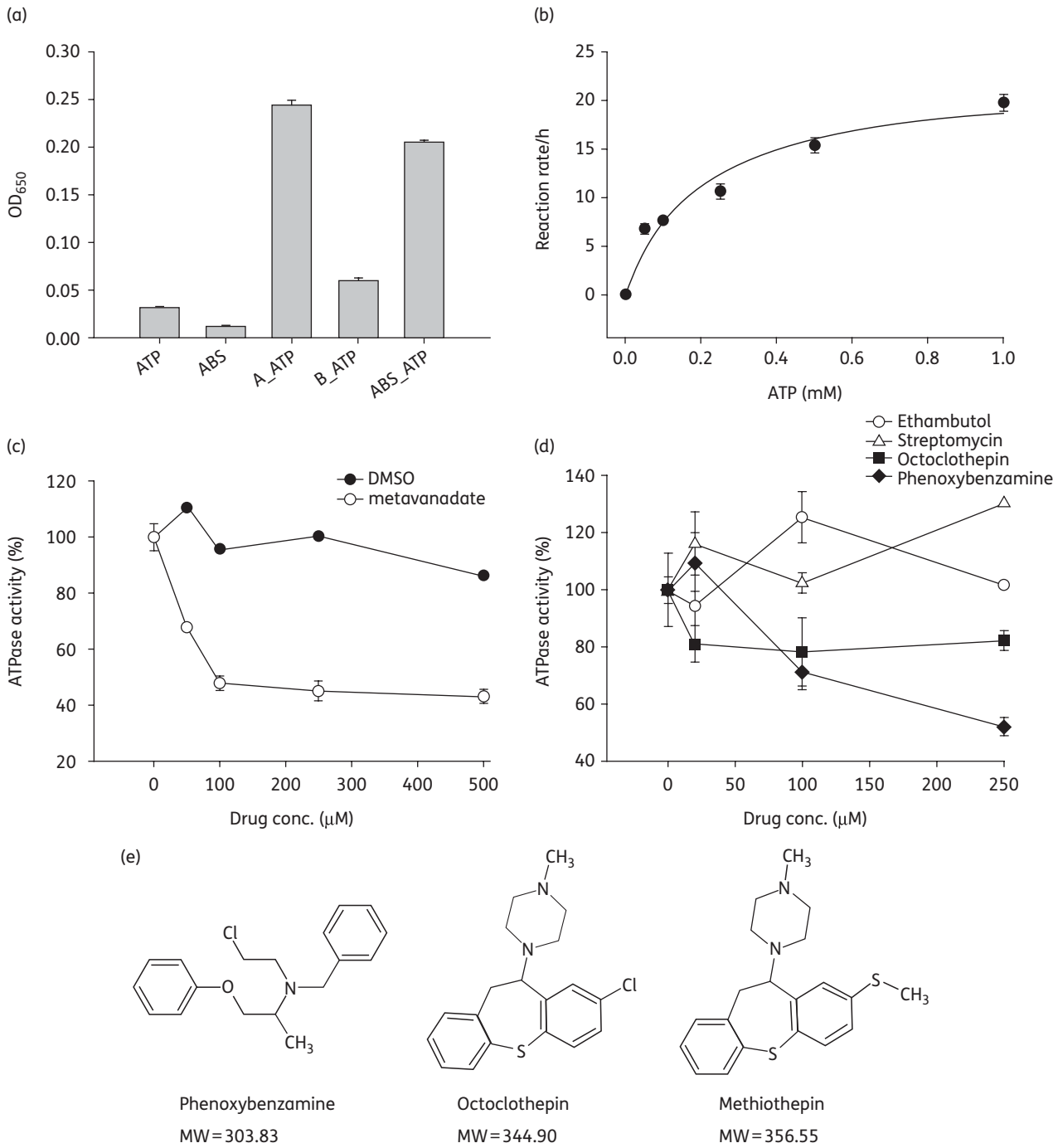

Figure 4. (a) ATP hydrolysis in the presence of ParA, ParB and ParABS ($n=2$). (b) Saturation curve showing the relationship between the concentration of ATP and the rate of reaction ($n=10$). Each reaction was performed using 3 μg of ParA and the data conformed to the Michaelis–Menten equation. (c) ATPase activity of ParA in the presence of DMSO and sodium metavanadate ($n=3$). While DMSO had a minimal effect, addition of 50 μM and 100 μM metavanadate reduced the ATPase activity by approximately 30% and 50%, respectively. (d) ATPase activity of ParA in the presence of ethambutol, streptomycin, phenoxybenzamine and octoclothepin ($n=2$). Addition of the standard tuberculosis drugs ethambutol and streptomycin did not cause a significant reduction in the ATPase activity of ParA, while phenoxybenzamine and octoclothepin decreased the activity of ParA ATPase by approximately 50% and 20%, respectively. Methiothepin decreased the ATPase activity of ParA to a similar level as octoclothepin (data not shown). All data points are normalized against spontaneous ATP decay and results are mean values of duplicates ± standard error. (e) Structural formula and molecular weight (MW) of phenoxybenzamine [*N*-benzyl-*N*-(2-chloroethyl)-1-phenoxypropan-2-amine], octoclothepin [1-(3-chloro-5,6-dihydrobenzo[b][1]benzothiepin-5-yl)-4-methylpiperazine] and methiothepin [1-methyl-4-(3-methylsulfanyl-5,6-dihydrobenzo[b][1]benzothiepin-5-yl)piperazine].

Table 1. Kinetic parameters of the ATPase activity of ParA from *M. tuberculosis*

Compound	Compound concentration (μM)	K_{cat} (h^{-1})	K_m (mM)
ParA (uninhibited)	—	22.57 ± 2.64	0.2 ± 0.07
Sodium metavanadate[a]	500	29.76 ± 4.16	0.86 ± 0.21
Phenoxybenzamine	250	6.38 ± 0.59	0.44 ± 0.09
Octoclothepin	250	21.01 ± 0.71	0.45 ± 0.02

[a]The known P-loop ATPase inhibitor sodium metavanadate was used as a control.

and streptomycin had no significant effect on the ATPase activity of ParA (Figure 4d).

Predicted interactions between inhibitors and the ATPase domain of ParA

A homology model of *M. tuberculosis* ParA was generated based on the template structure of Soj from *Thermus thermophilus*.[38] This was used to dock in ADP (Figure 5a), the (R)- and (S)-isomers of phenoxybenzamine (Figure 5b), and (±-)-octoclothepin maleate (Figure 5c). The analysis showed that phenoxybenzamine and (±)-octoclothepin maleate bind in the same pocket as the ADP molecule. Both isomers of phenoxybenzamine form a hydrogen bond between the ether oxygen atom and the -OH group of threonine-100 (Figure 5b). The benzylamine ($C_6H_5CH_2N$-R_2) group binds to a relatively hydrophobic pocket lined by alanine-130, proline-308 and threonine-99. The remainder of the binding site is lined by threonine-269, methionine-270, isoleucine-198, tyrosine-327 and serine-305. (±)-Octoclothepin maleate is bound to the ligand binding site with the chloride group binding to the hydrophobic pocket centred at alanine-130 (Figure 5c). Methiothepin mesylate binds in an almost identical fashion to (±)-octoclothepin maleate with the methyl sulfane group binding to the hydrophobic pocket centred at alanine-130 (data not shown). For all three ParA inhibitors, an aromatic ring occupies a similar position to the adenine ring of ADP. The *in silico* analyses provided evidence that the compounds phenoxybenzamine, methiothepin and octoclothepin dock in the ADP-binding site of ParA.

Inhibition of mycobacterial growth by ParA inhibitors

The effect of the ParA inhibitors on the cell morphology of *M. smegmatis* was tested. Induction of *parA* antisense in *M. smegmatis* resulted in a minor but statistically significant increase in cell length (5.08 ± 1.45 to 6.8 ± 1.3 μm). Cells expressing *parA* antisense also appeared to exhibit a higher number of chromosomal foci with respect to control *M. smegmatis*/pMindGFP cells (Figure 6a and b). Incubation of the *parA* antisense-expressing strain in the presence of 20 μM phenoxybenzamine or octoclothepin resulted in a large increase in cell length to 11.36 ± 2.6 and 14.78 ± 3.18 μm, respectively, and an observable increase in chromosomal foci number (Figure 6c and d). On the other hand, the compounds at 20 μM did not induce an elongated cell phenotype in the absence of

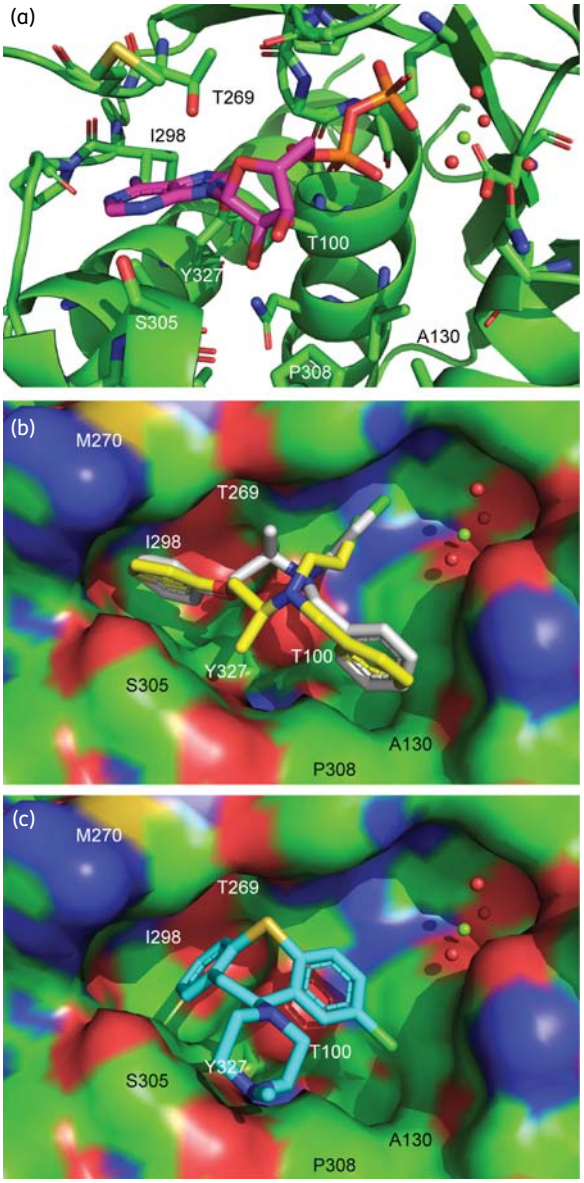

Figure 5. *In silico* studies of inhibitors on ParA of *M. tuberculosis*. (a) Binding site of the ParA homology model (green ribbon) with ADP (carbon, magenta; nitrogen, blue; oxygen, red); ADP from pdb2bej superimposed onto model. (b) Docking results showing superposition of (R) and (S) isomers of phenoxybenzamine on ParA of *M. tuberculosis*. (c) Octoclothepin (cyan carbons) docked into the ligand binding site. The *in silico* analysis showed that phenoxybenzamine and (±)-octoclothepin maleate bind in the same pocket as the ADP molecule. Surface representation of the ligand binding site shown as a surface. All representations are in the same orientation. All figures were generated using PyMOL. This figure appears in colour in the online version and in black and white in the print version of *JAC*.

parA antisense (data not shown). In terms of an effect on growth, under nutrient-rich conditions phenoxybenzamine had no detectable effect on the growth of *M. smegmatis* up to a concentration of 1000 μM (340 mg/L). In contrast, octoclothepin gave an MIC_{90} of 61.16 μM (28 mg/L) (Table 2). *M. smegmatis*

Table 2. Measurement of the bacteriostatic activity of the ParA ATPase inhibitors towards mycobacterial species

Strain	Culture conditions	MIC_{90}(μM)	
		phenoxybenzamine	octoclothepin
M. smegmatis mc^{2}155[a]	nutrient rich	≥1000	61.16
	C limitation	500.7	78.92
	N limitation	132.2	38.2
M. bovis BCG[a]	nutrient-rich	≥1000	37.88
M. tuberculosis H37Ra	nutrient-rich	≥1000	56.88
M. tuberculosis H37Rv	nutrient-rich	≥1000	34.7
M. tuberculosis CDC1551	nutrient-rich	≥1000	17.4

C limitation, carbon-limited growth conditions; N limitation, nitrogen-limited growth conditions.
[a]*M. smegmatis* and *M. bovis* BCG strains used were GFP-labelled.

exhibited sensitivity to phenoxybenzamine when grown under nitrogen limitation, i.e. MIC_{10} of 132.2 μM (45 mg/L). The MIC_{90} for octoclothepin also decreased under nitrogen limitation, i.e. 38.2 μM or 18 mg/L (Table 2). The effect of the ParA inhibitors on the growth of other species of mycobacteria was also tested grown under nutrient-rich conditions. Again, phenoxybenzamine did not exhibit detectable activity under these conditions. Octoclothepin, on the other hand, was active against *M. bovis* BCG and avirulent and virulent strains of *M. tuberculosis*, with the lowest MIC_{90} value obtained for strain CDC1551, 17.4 μM or 8 mg/L (Table 2).

Discussion

The spread of antibiotic resistance in human pathogens has necessitated the identification of new cellular targets and their cognate inhibitors for the development of alternative antimicrobial drugs.[39,40] One approach used in the identification of drug targets is the determination of a minimal gene set for a pathogen. A minimal gene set consists of genes that are essential and sufficient for sustaining a living organism under favourable

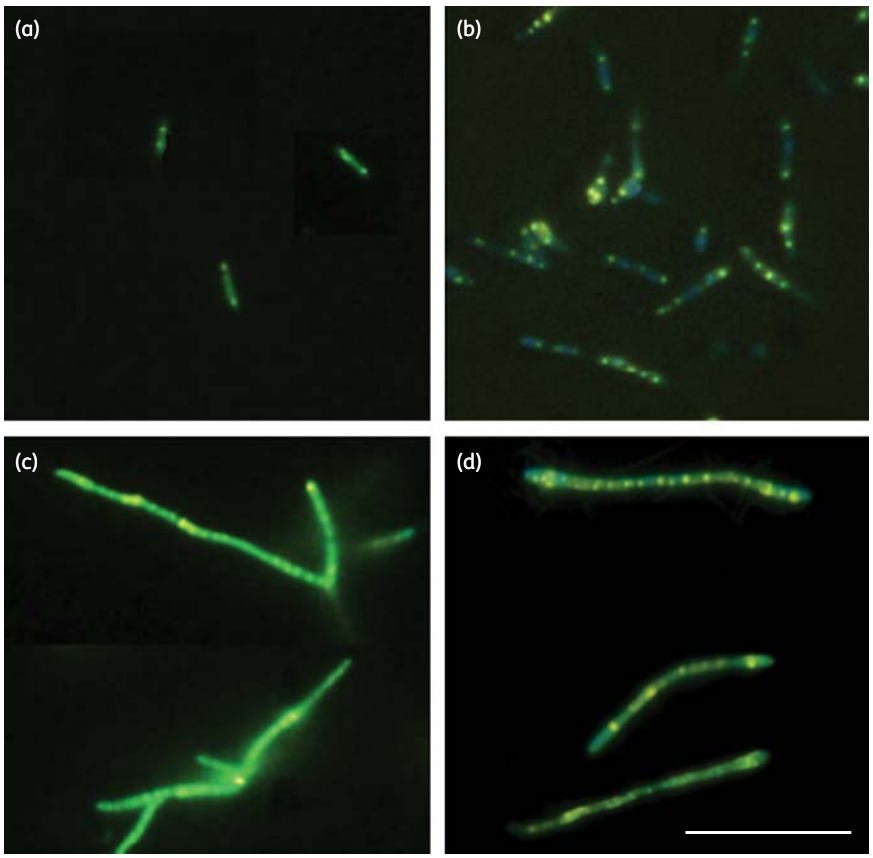

Figure 6. (a) *M. smegmatis*/pMindGFP and (b) *M. smegmatis*/pMind6969GFP cells under nitrogen-limited conditions in the presence of 0.02 mg/L tetracycline. *M. smegmatis*/pMindGFP cells show a couple of chromosomal foci per cell while *M. smegmatis*/pMind6969GFP cells contain multiple chromosomal loci along the length of the cells. *M. smegmatis*/pMind6969GFP cells under nitrogen limitation in the presence of 0.02 mg/L tetracycline and 20 μM (c) phenoxybenzamine and (d) octoclothepin. Both (c) and (d) show elongated cells with multiple foci along the length of the cells. The lengths of 100 cells were measured for each culture and from (a) to (d) were 5.08±1.45, 6.8±1.3, 11.36±2.6 and 14.78±3.18 μm, respectively. Images were taken with a ×100 oil-immersion lens. The scale bar is 10 μm and applies to all images. This figure appears in colour in the online version and in black and white in the print version of *JAC*.

conditions with all requisite nutrients provided and in the absence of environmental stress.[41] Chemical blocking of an essential gene product may provide an effective way to inhibit growth of a pathogen. In earlier work by Sassetti *et al.*,[25] *M. tuberculosis* H37Rv was mutated by high-density transposon mutagenesis and the loci containing transposon insertions were established. Transposon insertions were not obtained for 614 of the 3995 known *M. tuberculosis* genes,[17] which raised the possibility that many of these genes are essential for mycobacterial growth.

In this work, we selected the chromosomal partitioning *par* system as a potential drug target based on the transposon mutagenesis findings that *parA* (Rv3918c) and *parB* (Rv3917c) may be indispensable in *M. tuberculosis*.[25] Furthermore, orthologues of *parA* are also essential in a range of other bacterial species from our analysis of the Database of Essential Genes (http://tubic.tju.edu.cn/deg/). The role of the *par* system has been best characterized for plasmid partitioning, whereby DNA segregation is mediated by the plasmid-encoded proteins ParA and ParB and a *cis*-acting centromere-like partition site, *pars*.[19,42] Plasmid partitioning is an active process that requires the separation and maintenance of replicated DNA at subcellular locations.[43] Energy is derived from the ATPase activity of ParA, which is recruited to the partition nucleoprotein complex (ParB–*parS*) via its interaction with ParB.[44] ParB binds the centromere-like *parS* sites and membrane-bound proteins.[45,46] This process aligns the newly replicated plasmid towards the cell poles to ensure equipartitioning during division. Chromosomally encoded orthologues of the *par* system are understood to function in a similar manner to the plasmid *par* system and participate in the segregation of the newly formed daughter chromosomes during cell division.[19]

In this study, antisense expression of *parA* and *parB* was used to examine their essentiality in *M. smegmatis*. Antisense gene expression has been used previously to repress essential gene expression in a number of bacterial species, including *M. smegmatis*,[29,47,48] *M. tuberculosis*,[49] *Staphylococcus aureus*[50,51] and *Streptococcus mutans*.[52] To detect induction of the gene antisense, a *gfp* reporter gene was cloned downstream of the antisense fragment. Only the expression of *parA* antisense was found to hinder the growth of *M. smegmatis*, indicating that ParA, but not ParB, may be essential in *M. smegmatis* (Figure 3). Other researchers have shown that *parB* can be inactivated in *M. smegmatis*,[53] indicating that *parB* is not essential in this species.

Expression of *parA* antisense was then used in the identification of inhibitors of mycobacterial growth from chemical libraries. An antisense differential sensitivity whole-cell approach similar to what has previously been applied to the identification of specific inhibitors of FabI[36] and FabF[54–57] in *Staphylococcus aureus* was used. Screens were carried out under three different growth conditions. It has been established previously that mycobacteria reduce transcription of genes involved in processes such as energy metabolism, translation and cell division upon nutrient starvation.[58] This global shift in gene expression can affect the susceptibility of mycobacterial cells to antibacterial agents. Indeed, we have previously shown in our laboratory that nutrient limitation significantly changes the activity profile of a chemical library and can cause substantial shifts in the MICs of some compounds.[31] Furthermore, it has been demonstrated that transcription of *parA* is down-regulated upon nutrient starvation in *M. tuberculosis*.[58] This effect on *parA* expression would be expected to modulate the sensitivity of mycobacteria to compounds that target ParA, and hence the screens were performed under nutrient-limited as well as nutrient-rich conditions.

Parallel screens with a reference strain expressing antisense RNA of a putative essential gene, not involved in the cell division process, were performed. Compounds that inhibited growth of both strains were excluded, whereas 44 distinct compounds displayed differential activity towards the *parA* antisense strain. Of these, seven compounds also caused cell elongation, indicating a possible effect on cell division or chromosomal partitioning. These latter compounds were selected for validation against the purified ParA protein from *M. tuberculosis*. Three compounds, phenoxybenzamine, octoclothepin and methiothepin, were found to inhibit the ATPase activity of *M. tuberculosis* ParA *in vitro* (Figure 4). Their interaction with ParA was supported by *in silico* analysis, which indicated that these compounds bind within the ATPase site of ParA (Figure 5).

The effects of phenoxybenzamine and octoclothepin on cell morphology and growth were examined in *M. smegmatis*. In the presence of *parA* antisense, both compounds resulted in a significantly elongated cell phenotype and an increase in the amount of nucleation visible (Figure 6). A change in cell morphology was not evident when the compounds were administered in the absence of *parA* antisense; however, the compounds inhibited the growth of *M. smegmatis* (Table 2). Under the three culture conditions tested, octoclothepin was the more active of the two compounds. Phenoxybenzamine exhibited no inhibitory activity under nutrient-rich conditions, but was active against *M. smegmatis* under nitrogen limitation (Table 2). The compounds were also tested against slow-growing mycobacteria. Again, phenoxybenzamine was inactive against all strains when tested under nutrient-rich conditions. We are currently developing a nutrient-limitation model for *M. bovis* BCG and *M. tuberculosis* to examine whether nutrient deprivation alters the activity of phenoxybenzamine in these species as was seen in *M. smegmatis*. On the other hand, octoclothepin was active against all of the slow-growing mycobacterial strains tested (Table 2). Although octoclothepin exhibited lower inhibitory activity towards purified ParA *in vitro* with respect to phenoxybenzamine, its higher activity against mycobacterial cells indicates that it may target other ATPases in the mycobacterial cell in addition to ParA.

Octoclothepin is an analogue of the piperazine derivative clozapine, which is used in the treatment of schizophrenia[59] under a variety of brand names including Denzapine and Zaponex. Clozapine is an agonist of a number of dopamine receptors such as the D_4 receptor,[60] but also acts as an antagonist of adrenergic and histaminergic receptors.[61] Previous *in silico* analyses of octoclothepin resulted in it being predicted to be non-antibacterial;[62,63] however, this study clearly demonstrates that it has anti-mycobacterial properties. Importantly, octoclothepin is active against virulent *M. tuberculosis* (Table 2) and its measured level of toxicity in mice—an oral 50% lethal dose (LD_{50}) of 78 mg/kg—compares well with that of isoniazid, 133 mg/kg (ChemIDplus Advanced). Therefore, this compound deserves further attention as a possible anti-tubercular agent. Methiothepin has been detected in a high-throughput growth inhibition assay with *M. tuberculosis* H37Rv performed by the Southern Research Institute (data available at http://pubchem.ncbi.nlm.nih.gov/);

however, an antibacterial cellular target for this compound has not been described to date.

Phenoxybenzamine, marketed as Dibenzyline® by Wellspring Pharmaceutical Corporation, is a haloalkylamine used in the treatment of hypertension.[64] It is also used in the treatment of benign prostatic hyperplasia.[65] It acts by covalently binding to and blocking $\alpha 1$ and $\alpha 2$ adrenergic receptors in vascular smooth muscle, resulting in systemic vasodilation. Phenoxybenzamine administered orally is well tolerated in rats (LD_{50} of 2500 mg/kg), mice (LD_{50} of 1536 mg/kg) and guinea pigs (LD_{50} of 500 mg/kg).[66] An earlier study found that pre-treatment of mice with phenoxybenzamine reduced pneumococcal and staphylococcal sepsis mortalities through decreased vasoconstriction,[67] but we have been unable to find reports of direct antibacterial activity for phenoxybenzamine.

In summary, we have demonstrated that screening using differential antisense sensitivity can identify specific inhibitors of mycobacterial cellular targets from a large number of library compounds. Using this approach we have identified inhibitors of the ParA ATPase, an essential chromosome partitioning protein, of *M. tuberculosis*. These compounds represent the first reported inhibitors identified for this protein in mycobacteria and may provide a basis for the further development of ParA as a cell division target for anti-tubercular drugs. One compound in particular, octoclothepin, inhibits the growth of virulent *M. tuberculosis* and will be the subject of future structure–activity studies.

Acknowledgements

We would like to thank Dr Joanna Kirman for helpful advice and Mudassar Altaf for compound MICs for avirulent strains BCG and H37Ra.

Funding

We received support from the Health Research Council of New Zealand (grant 07/379), the Wellington Medical Research Foundation (grant 2009/184) and the University Research Fund, Victoria University of Wellington (grant 26211/1496). We also received support from the New Zealand Foundation for Research, Science and Technology (grant IIOF) and Tertiary Education Commission, and the National Institutes of Health, USA (grants AI36973, AI37856 and AI079590).

Transparency declarations

None to declare.

References

1 Berman HM, Westbrook J, Feng Z *et al*. The Protein Data Bank. *Nucleic Acids Res* 2000; **28**: 235–42.

2 Hershkovitz I, Donoghue HD, Minnikin DE *et al*. Detection and molecular characterization of 9,000-year-old *Mycobacterium tuberculosis* from a Neolithic settlement in the Eastern Mediterranean. *PLoS ONE* 2008; **3**: e3426.

3 WHO. *World Health Organization Report 2009. Global Tuberculosis Control: Epidemiology; Strategy; Financing*. http://www.who.int/tb/publications/global_report/2009/pdf/full_report.pdf (10 August 2010, date last accessed).

4 IUATLD. *International Union Against Tuberculosis and Lung Disease, Anti-Tuberculosis Drug Resistance in the World, Report No. 4*. 2008.

5 WHO. *World Health Organization and the Stop TB Partnership. Building on and Enhancing DOTS to Meet the TB-Related Millennium Development Goals*. http://www.who.int/tb/publications/2006/stop_tb_strategy.pdf (10 August 2010, date last accessed).

6 Espinal MA, Kim SJ, Suarez PG *et al*. Standard short-course chemotherapy for drug-resistant tuberculosis: treatment outcomes in 6 countries. *JAMA* 2000; **283**: 2537–45.

7 CDC. Emergence of *Mycobacterium tuberculosis* with extensive resistance to second-line drugs worldwide, 2000–2004. *MMWR Morb Mortal Wkly Rep* 2006; **55**: 301–5.

8 Matteelli A, Migliori GB, Cirillo D *et al*. Multidrug-resistant and extensively drug-resistant *Mycobacterium tuberculosis*: epidemiology and control. *Expert Rev Anti Infect Ther* 2007; **5**: 857–71.

9 WHO. *World Health Organization Press Release, 5 September 2006. WHO Concern Over Extensive Drug Resistant TB Strains That Are Virtually Untreatable*. http://www.who.int/mediacentre/news/notes/2006/np23/en/index.html (10 August 2010, date last accessed).

10 WHO. *Multidrug and extensively drug-resistant TB (M/XDR-TB): 2010 global report on surveillance and response*. http://www.whqlibdoc.who.int/publications/2010/9789241599191_eng.pdf (10 August 2010, date last accessed).

11 WHO. *World Health Organization and the Stop TB Partnership. Global Plan to Stop TB*. http://www.who.int/tb/features_archive/global_plan_to_stop_tb/en/index.html (10 August 2010, date last accessed).

12 Wade MM, Zhang Y. Mechanisms of drug resistance in *Mycobacterium tuberculosis*. *Front Biosci* 2004; **9**: 975–94.

13 Chopra P, Meena LS, Singh Y. New drug targets for *Mycobacterium tuberculosis*. *Indian J Med Res* 2003; **117**: 1–9.

14 Hasan S, Daugelat S, Rao PS *et al*. Prioritizing genomic drug targets in pathogens: application to *Mycobacterium tuberculosis*. *PLoS Comput Biol* 2006; **2**: e61.

15 Mdluli K, Spigelman M. Novel targets for tuberculosis drug discovery. *Curr Opin Pharmacol* 2006; **6**: 459–67.

16 Cole ST, Brosch R, Parkhill J *et al*. Deciphering the biology of *Mycobacterium tuberculosis* from the complete genome sequence. *Nature* 1998; **393**: 537–44.

17 Camus JC, Pryor MJ, Medigue C *et al*. Re-annotation of the genome sequence of *Mycobacterium tuberculosis* H37Rv. *Microbiology* 2002; **148**: 2967–73.

18 Errington J, Daniel RA, Scheffers DJ. Cytokinesis in bacteria. *Microbiol Mol Biol Rev* 2003; **67**: 52–65, table of contents.

19 Leonard TA, Moller-Jensen J, Lowe J. Towards understanding the molecular basis of bacterial DNA segregation. *Philos Trans R Soc Lond B Biol Sci* 2005; **360**: 523–35.

20 Ryan KR, Shapiro L. Temporal and spatial regulation in prokaryotic cell cycle progression and development. *Annu Rev Biochem* 2003; **72**: 367–94.

21 Margalit DN, Romberg L, Mets RB *et al*. Targeting cell division: small-molecule inhibitors of FtsZ GTPase perturb cytokinetic ring assembly and induce bacterial lethality. *Proc Natl Acad Sci USA* 2004; **101**: 11821–6.

22 Projan SJ. New (and not so new) antibacterial targets–from where and when will the novel drugs come? *Curr Opin Pharmacol* 2002; **2**: 513–22.

23 White EL, Southworth K, Ross L *et al*. A novel inhibitor of *Mycobacterium tuberculosis* pantothenate synthetase. *J Biomol Screen* 2007; **12**: 100–5.

24 Bhat J, Rane R, Solapure SM *et al*. High-throughput screening of RNA polymerase inhibitors using a fluorescent UTP analog. *J Biomol Screen* 2006; **11**: 968–76.

25 Sassetti CM, Boyd DH, Rubin EJ. Genes required for mycobacterial growth defined by high density mutagenesis. *Mol Microbiol* 2003; **48**: 77–84.
26 Smeulders MJ, Keer J, Speight RA *et al*. Adaptation of *Mycobacterium smegmatis* to stationary phase. *J Bacteriol* 1999; **181**: 270–83.
27 O'Toole R, Smeulders MJ, Blokpoel MC *et al*. A two-component regulator of universal stress protein expression and adaptation to oxygen starvation in *Mycobacterium smegmatis*. *J Bacteriol* 2003; **185**: 1543–54.
28 Belisle JT, Mahaffey SB, Hill PJ. Isolation of *Mycobacterium* species genomic DNA. In: Parish T, Brown AC, eds. *Mycobacteria Protocols*. 2nd Edn. New York, NY: Humana Press. 2008; 1–12.
29 Blokpoel MC, Murphy HN, O'Toole R *et al*. Tetracycline-inducible gene regulation in mycobacteria. *Nucleic Acids Res* 2005; **33**: e22.
30 Bourn WR, Jansen Y, Stutz H *et al*. Creation and characterisation of a high-copy-number version of the pAL5000 mycobacterial replicon. *Tuberculosis* 2007; **87**: 481–8.
31 Miller CH, Nisa S, Dempsey S *et al*. Modifying culture conditions in chemical library screening identifies alternative inhibitors of mycobacteria. *Antimicrob Agents Chemother* 2009; **53**: 5279–83.
32 Studier FW. Protein production by auto-induction in high-density shaking cultures. *Protein Expr Purif* 2005; **41**: 207–34.
33 Eswar N, Webb B, Marti-Renom MA *et al*. Comparative protein structure modeling using Modeller. *Curr Protoc Bioinformatics* 2006; Supplement 15: 5.6.1–30.
34 Cole JC, Murray CW, Nissink JW *et al*. Comparing protein-ligand docking programs is difficult. *Proteins* 2005; **60**: 325–32.
35 McQuade TJ, Shallop AD, Sheoran A *et al*. A nonradioactive high-throughput assay for screening and characterization of adenylation domains for nonribosomal peptide combinatorial biosynthesis. *Anal Biochem* 2009; **386**: 244–50.
36 Ji Y, Yin D, Fox B *et al*. Validation of antibacterial mechanism of action using regulated antisense RNA expression in Staphylococcus aureus. *FEMS Microbiol Lett* 2004; **231**: 177–84.
37 Ebersbach G, Gerdes K. Plasmid segregation mechanisms. *Annu Rev Genet* 2005; **39**: 453–79.
38 Leonard TA, Butler PJ, Lowe J. Bacterial chromosome segregation: structure and DNA binding of the Soj dimmer—a conserved biological switch. *EMBO J* 2005; **24**: 270–82.
39 Charles PG, Grayson ML. The dearth of new antibiotic development: why we should be worried and what we can do about it. *Med J Aust* 2004; **181**: 549–53.
40 Alanis AJ. Resistance to antibiotics: are we in the post-antibiotic era? *Arch Med Res* 2005; **36**: 697–705.
41 Koonin EV. How many genes can make a cell: the minimal-gene-set concept. *Annu Rev Genomics Hum Genet* 2000; **1**: 99–116.
42 Schumacher MA. Structural biology of plasmid segregation proteins. *Curr Opin Struct Biol* 2007; **17**: 103–9.
43 Lee PS, Grossman AD. The chromosome partitioning proteins Soj (ParA) and Spo0J (ParB) contribute to accurate chromosome partitioning, separation of replicated sister origins, and regulation of replication initiation in *Bacillus subtilis*. *Mol Microbiol* 2006; **60**: 853–69.
44 Hayes F, Barillà D. Assembling the bacterial segrosome. *Trends Biochem Sci* 2006; **31**: 247–50.
45 Bouet J-Y, Funnell BE. P1 ParA interacts with the P1 partition complex at parS and an ATP-ADP switch controls ParA activities. *EMBO J* 1999; **18**: 1415–24.
46 Surtees JA, Funnell BE. Plasmid and chromosome traffic control: how ParA and ParB drive partition. *Curr Top Dev Biol* 2003; **56**: 145–80.
47 Parish T, Stoker NG. Development and use of a conditional antisense mutagenesis system in mycobacteria. *FEMS Microbiol Lett* 1997; **154**: 151–7.
48 Ehrt S, Guo XV, Hickey CM *et al*. Controlling gene expression in mycobacteria with anhydrotetracycline and Tet repressor. *Nucleic Acids Res* 2005; **33**: e21.
49 Wu S, Howard ST, Lakey DL *et al*. The principal sigma factor *sigA* mediates enhanced growth of *Mycobacterium tuberculosis in vivo*. *Mol Microbiol* 2004; **51**: 1551–62.
50 Forsyth RA, Haselbeck RJ, Ohlsen KL *et al*. A genome-wide strategy for the identification of essential genes in Staphylococcus aureus. *Mol Microbiol* 2002; **43**: 1387–400.
51 Ji Y, Zhang B, Van SF *et al*. Identification of critical staphylococcal genes using conditional phenotypes generated by antisense RNA. *Science* 2001; **293**: 2266–9.
52 Wang B, Kuramitsu HK. Inducible antisense RNA expression in the characterization of gene functions in Streptococcus mutans. *Infect Immun* 2005; **73**: 3568–76.
53 Jakimowicz D, Brzostek A, Rumijowska-Galewicz A *et al*. Characterization of the mycobacterial chromosome segregation protein ParB and identification of its target in *Mycobacterium smegmatis*. *Microbiology* 2007; **153**: 4050–60.
54 Ondeyka JG, Zink DL, Young K *et al*. Discovery of bacterial fatty acid synthase inhibitors from a Phoma species as antimicrobial agents using a new antisense-based strategy. *J Nat Prod* 2006; **69**: 377–80.
55 Wang J, Kodali S, Lee SH *et al*. Discovery of platencin, a dual FabF and FabH inhibitor with *in vivo* antibiotic properties. *Proc Natl Acad Sci USA* 2007; **104**: 7612–6.
56 Wang J, Soisson SM, Young K *et al*. Platensimycin is a selective FabF inhibitor with potent antibiotic properties. *Nature* 2006; **441**: 358–61.
57 Young K, Jayasuriya H, Ondeyka JG *et al*. Discovery of FabH/FabF inhibitors from natural products. *Antimicrob Agents Chemother* 2006; **50**: 519–26.
58 Betts JC, Lukey PT, Robb LC *et al*. Evaluation of a nutrient starvation model of *Mycobacterium tuberculosis* persistence by gene and protein expression profiling. *Mol Microbiol* 2002; **43**: 717–31.
59 Tehan BG, Lloyd EJ, Wong MG. Molecular field analysis of clozapine analogs in the development of a pharmacophore model of antipsychotic drug action. *J Mol Graph Model* 2001; **19**: 417–26, 468.
60 Leysen JE, Janssen PM, Schotte A *et al*. Interaction of antipsychotic drugs with neurotransmitter receptor sites *in vitro* and *in vivo* in relation to pharmacological and clinical effects: role of 5HT2 receptors. *Psychopharmacology (Berl)* 1993; **112**: S40–54.
61 Metysová JMJ, Dlabac A, Kazdová E, Valchár M. Pharmacological properties of a potent neuroleptic drug octoclothepin. *Acta Biol Med Ger* 1980; **39**: 723–40.
62 Tomás-Vert F, Pérez-Giménez F, Salabert-Salvador MT *et al*. Artificial neural network applied to the discrimination of antibacterial activity by topological methods. *J Mol Struct (Theochem)* 2000; **504**: 249–59.
63 Cronin MTD, Aptula AO, Dearden JC *et al*. Structure-based classification of antibacterial activity. *J Chem Inf Comput Sci* 2002; **42**: 869–78.
64 Guzzetta NA. Phenoxybenzamine in the treatment of hypoplastic left heart syndrome: a core review. *Anesth Analg* 2007; **105**: 312–5.
65 Caine M, Perlberg S, Meretyk S. A placebo-controlled double-blind study of the effect of phenoxybenzamine in benign prostatic obstruction. *Br J Urol* 1978; **50**: 551–4.
66 Barnes CD, Eltherington LG. *Drug Dosages in Laboratory Animals—A Handbook*. Berkeley, USA: University of California Press, 1973.
67 Robson HG, Cluff LE. Experimental pneumococcal and staphylococcal sepsis: effects of hydrocortisone and phenoxybenzamine upon mortality rates. *J Clin Invest* 1966; **45**: 1421–32.
68 Dong X, Stothard P, Forsythe IJ *et al*. PlasMapper: a web server for drawing and auto-annotating plasmid maps. *Nucl Acids Res* 2004; **32**: W660–4.